Journal of Nuclear Materials 385 (2009) 288–293

Contents lists available at ScienceDirect

Journal of Nuclear Materials

journal homepage: www.elsevier.com/locate/jnucmat

Oxidation behavior of Incoloy 800 under simulated supercritical water conditions

M. Fulger [a,*], D. Ohai [a], M. Mihalache [a], M. Pantiru [a], V. Malinovschi [b]

[a] *Institute for Nuclear Research Pitesti, POB 78, Campului Street, No. 1, 115400 Mioveni, Romania*
[b] *University of Pitesti, Research Center for Advanced Materials, Targul din Vale Street, No. 1, 110040 Pitesti, Romania*

ARTICLE INFO

PACS:
28.41.Qb
81.65.Mq
68.55.J–
68.37.Hk
68.37.Yz

ABSTRACT

For a correct design of supercritical water-cooled reactor (SCWR) components, data regarding the behavior of candidate materials in supercritical water are necessary. Corrosion has been identified as a critical problem because the high temperature and the oxidative nature of supercritical water may accelerate the corrosion kinetics. The goal of this paper is to investigate the oxidation behavior of Incoloy 800 exposed in autoclaves under supercritical water conditions for up to 1440 h. The exposure conditions (thermal deaerated water, temperatures of 723, 773, 823 and 873 K and a pressure of 25 MPa) have been selected as relevant for a supercritical power plant concept. To investigate the structural changes of the oxide films, X-ray diffraction (XRD), scanning electron microscopy (SEM), energy dispersive X-ray spectrometry (EDX) and electrochemical impedance spectroscopy (EIS) analyses were used. Results show changes in the oxides chemical composition, microstructure and thickness versus testing conditions (pressure, temperature and time). The oxide films are composed of two layers: an outer layer enriched in Fe oxide and an inner layer enriched in Cr and Ni oxides corresponding to small cavities supposedly due to internal oxidation.

1. Introduction

Supercritical water-cooled reactors (SCWRs) are promising advanced nuclear systems due their high thermal efficiency and considerable plant simplification. One of the major issues is to propose performant materials for the fuel claddings and the core components in the SCWR [1]. Because the materials will be used under high pressurized water at temperatures above the thermodynamic critical point of water, the requirements for cladding materials are: good mechanical properties, corrosion resistance, resistance to neutron irradiation, low susceptibility to stress corrosion cracking and microstructural stability [2]. Nickel-based alloys were selected as promising material based on experimental results of corrosion tests and mechanical tests before irradiation [3]. These alloys show a high tendency to form a protective oxide film in water at high temperatures. Based on its advantages such as high strength and corrosion resistance at high temperatures, Incoloy 800 (a high nickel alloy) is a candidate for Generation IV supercritical water-cooled nuclear plant design [4]. The present work aims at evaluating the general corrosion behavior of Incoloy 800 tubes exposed under supercritical water conditions for up to 1440 h. Gravimetry, optical microscopy, scanning electron microscopy/energy dispersion X-ray spectroscopy (SEM/EDS), X-ray diffraction (XRD) and electrochemical impedance spectroscopy (EIS) were used to analyze oxide growth and stability.

2. Experimental

The Incoloy 800 tube (13.9 mm outside diameter and 0.6 mm wall thickness) was cut into 10 mm long pieces, polished with grit papers and cleaned ultrasonically. The chemical composition of the studied material is given in Table 1. Samples were exposed in static autoclaves at four temperatures (723, 773, 823 and 873 K) under constant pressure of 25 MPa for periods up to 1440 h. Deionized water had a conductivity of 0.7 $\mu S\ cm^{-1}$ and its dissolved oxygen content was below 2 ppm (oxygen was released by thermal degassing at 373 K). The test solution working pH was ~6.3. Weight gains due to oxidation were measured using a balance providing a precision of ±0.001 mg.

The cross sections of the corrosion samples were analyzed with a SEM and energy dispersive X-ray spectroscopy (EDS) using a TESCAN VEGA II-LMU device. The oxidation kinetic was additionally evaluated by thermal gravimetric analysis (TGA) using a thermoanalyzer SETSYS EVOLUTION 24. Tests have been performed for 72 h, in flowing steam with Ar and 90% RH humidity.

Qualitative phase analysis has been done using a Rigaku ULTIMA IV X-ray diffractometer with θ–θ vertical goniometer. X-ray diffraction patterns have been acquired in symmetrical geometry using multilayer parallel-beam method. The disposal of oxides in layer has been evaluated from X-ray diffraction patterns acquired

---

* Corresponding author. Tel.: +40 0248 213 400x249; fax: +40 0248 262 449.
E-mail address: manuela.fulger@nuclear.ro (M. Fulger).

0022-3115/$ - see front matter © 2008 Elsevier B.V. All rights reserved.
doi:10.1016/j.jnucmat.2008.12.004

Table 1
Chemical composition of Incoloy 800.

Element	C	Al	Si	P	S	Ti	Cr	Mn	Fe	Ni	Cu
Fraction (wt%)	0.02	0.11	0.48	0.009	0.004	0.29	21.5	0.47	46.3	30.9	0.01

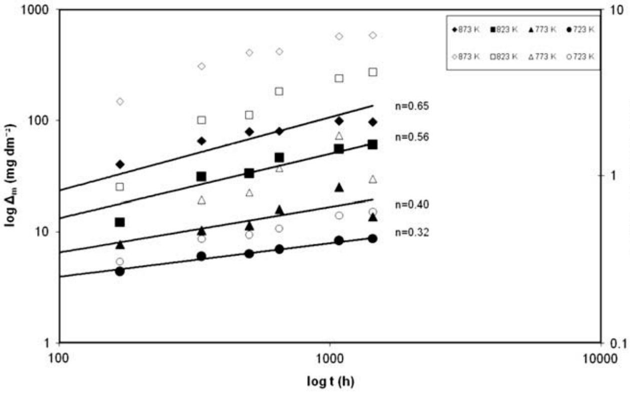

Fig. 1. Weight gain data (filled markers) and oxide thickness (opened markers) as a function of exposure time for Incoloy 800 exposed to supercritical water at 723, 773, 823 and 873 K under 25 MPa.

Table 2
Kinetic parameters for Incoloy 800 at different temperatures.

Temperature (K)	A' (mg dm^{-2} s^{-n})	n (–)	R^2 (–)	Kinetics
723	0.95	0.32	0.97	Cubic
773	0.94	0.40	0.91	Parabolic
823	0.92	0.56	0.98	Parabolic
873	1.19	0.65	0.97	Parabolic

in asymmetrical geometry with incidence angles α of 0.5° and 1.0°. The incident Cu Kα line $\lambda = 1.54178$ Å at 40 kV and 30 mA was used. The experimental conditions for qualitative phase analysis were: 5 s for each step, an angle range $2\theta = 22$–110° with a step of 0.05°. In order to analyze the oxides disposed into the surface layer, the experimental conditions were: 10 s for each step, range angle $2\theta = 22$–60° with 0.02° steps.

Electrochemical impedance spectroscopy measurements (EIS) were carried out at room temperature in a 0.05 M boric acid with 0.001 M borax solution (pH = 7.47) using a PAR 2273 device within the 10^{-1}–10^{5} Hz frequency range, at open circuit potential and room temperature.

3. Results and discussions

General corrosion tests were carried out by means of weight gain measurements after different exposure times in static autoclaves. Fig. 1 shows the dependence of weight gain on the corrosion test period for Incoloy 800 tube at four temperatures: 723, 773, 823 and 873 K at 25 MPa pressure. The corrosion kinetics at different temperatures follows different trends in time.

Since the testing time was much shorter than the service lifetime of nuclear reactors, an extrapolation based on fitting available experimental data was performed to provide an idea of trends in oxide growth. The experimental weight gain data (Δm) can be fitted using the following equation:

$$\Delta m = Ae^{(Q/k_BT)}t^n = A't^n, \tag{1}$$

where A and A' are constants, Q is the activation energy for oxidation, T is the temperature in Kelvin, t is the exposure time, k_B is the Boltzman constant and n is the time exponent. The fitting curves for each set of data are shown in Fig. 1 and the corresponding time exponent values and the A' values are presented in Table 2. It is important to note that the trends are based on limited experimental data set.

The results indicate that, at 723 K, the weight gain exhibited cubic growth kinetic ($n = 0.32$) whereas at 773, 823 and 873 K the

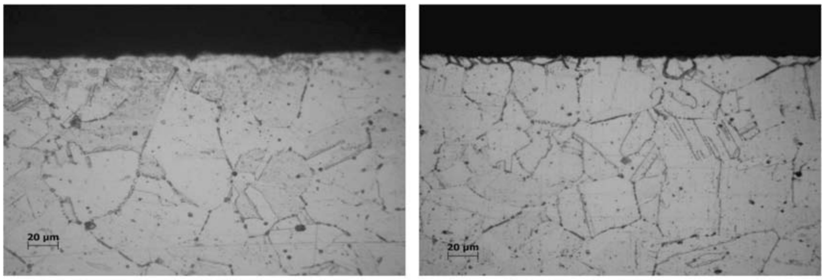

(a) Iy 800 as received (b) Iy 800 tested at 773 K for 1440 h

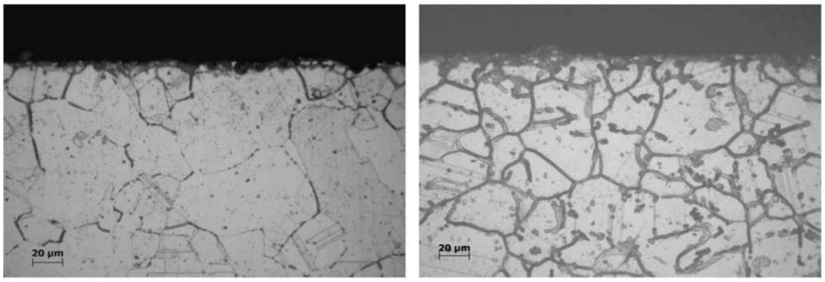

(c) Iy 800 tested at 823 K for 1440 h (d) Iy 800 tested at 873 K for 1440 h

Fig. 2. Grain boundary structure of Incoloy 800 tube: (a) as-received; (b) tested at 773 K for 1440 h; (c) tested at 823 K for 1440 h and (d) tested at 873 K for 1440 h.

growth kinetics were closer to parabolic ($n = 0.40, 0.56, 0.65$). The corrosion scale significantly increases with the temperature so the corrosion rate is highly temperature dependent.

The growth of oxide is generally considered to be from both outward migrations of iron ions to the surface, where they react with water molecules and the inward diffusion of oxygen ions to the metal–oxide interface, where they react with the metal [5]. Corrosion at 873 K and 25 MPa was fast, resulting in a 10-fold weight gain increase compared to the 723 K weight gain. The outer oxide layer thicknesses estimated for Incoloy 800 samples exposed at different temperatures, are shown in Fig. 1. The oxide thickness was calculated using a density of 5.2 g cm^{-3} for the magnetite (Fe_3O_4) [6]. From view of corrosion limits, at the highest temperature (873 K) and 25 MPa after 1440 h, Incoloy 800 tube showed an acceptable corrosion rate of about 2.0 μm a^{-1} (calculated from weight loss after descaling).

To reveal the grain boundary structure, the tubes were examined metallographically using electrolytic etching in oxalic acid. This examination was carried out before and after exposing in supercritical water. Investigations about grain size impact on the corrosion behavior in steam demonstrated that there is a marked improvement in the corrosion resistance of fine grained austenitic structure comparated to a coarse grained structure because a protective chromium oxide layer can be obtained through a finer grain size [7]. The 'as-received' Incoloy 800 tube samples show a microstructure consisting of the matrix austenite phase with large grain size (75 μm) as is shown in Fig. 2(a). The microstructure of samples tested at 723, 773 and 823 K contained similar sized grains after 1440 h whereas the samples exposed in water at 873 K presented thicker grain boundaries and a decreasing from 75 μm average to 60 μm average (Fig. 2(b)–(d)).

The surface morphology of the oxide layers on the samples after 1440 h is shown by SEM images (Fig. 3). With increasing temperature and exposure time, the topography and thickness of oxides changed on the surface of the samples in supercritical water. The oxide films were non-uniform with various thicknesses. A porous oxide structure was observed on the surface of samples exposed at the highest temperature (873 K) and the pores density was also noted to increase with exposure time. These pores are likely to act as pathways for transportation of oxygen. For samples exposed 1440 h at 873 K, the porosity of the external layer was about 20.3% compared to samples exposed 168 h at 873 K (3.8%) or compared to samples exposed 1440 h at 773 K (8.3%).

Optical microphotographs of scale cross sections are shown in Fig. 4(a) and (b) for Incoloy 800 tube after 168 and 1440 h exposure in water at 873 K. On the surface of these samples many cavities

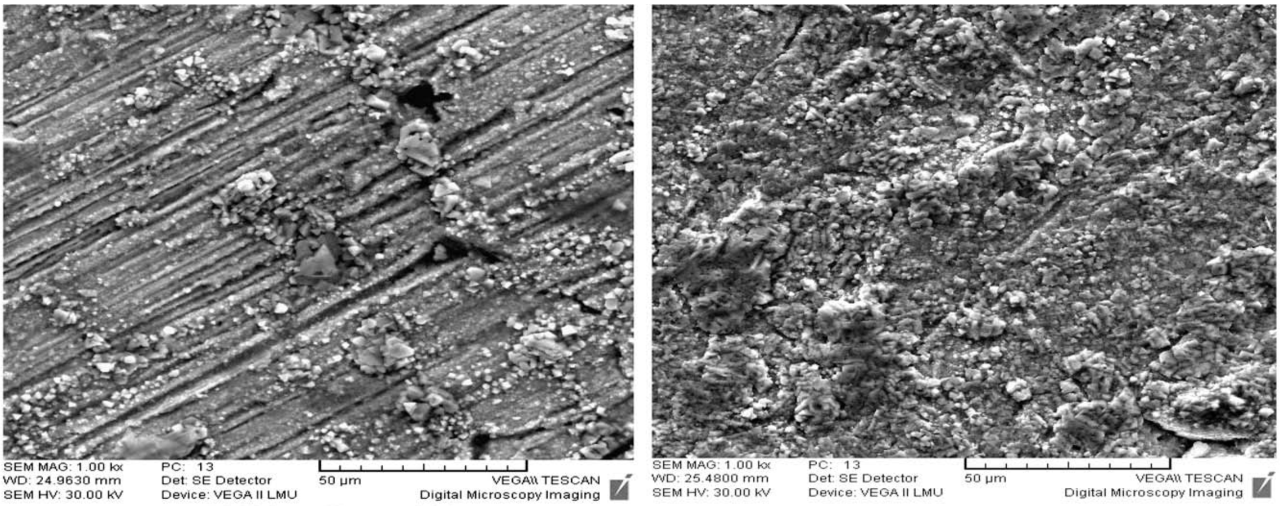

(a) 1440 h ; 723 K and 25 MPa

(c) 1440 h ; 823 K and 25 MPa

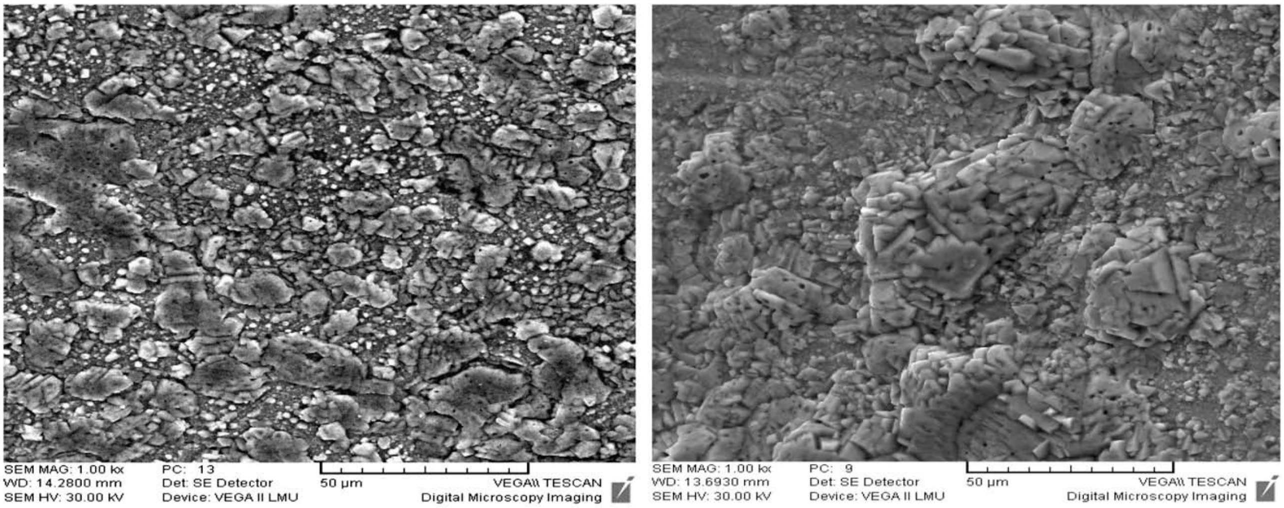

(b) **1440 h ; 773 K and 25 MPa**

(d)1440 h ; 873 K and 25 MPa

Fig. 3. SEM images of the surface morphologies of oxide layers on Incoloy 800 tested at: 723, 773, 823 and 873 K for 1440 h.

were observed. They are expected to be generated because of high concentration of oxygen in the water. The oxide layer thickness varied as is shown in optical microphotographs (Fig. 4). The samples exposed for a longer time (1440 h) presented larger outer oxide layers (3.1–12.3 μm) and larger inner oxide layers (13.6–21 μm) compared with samples exposed at the same temperature

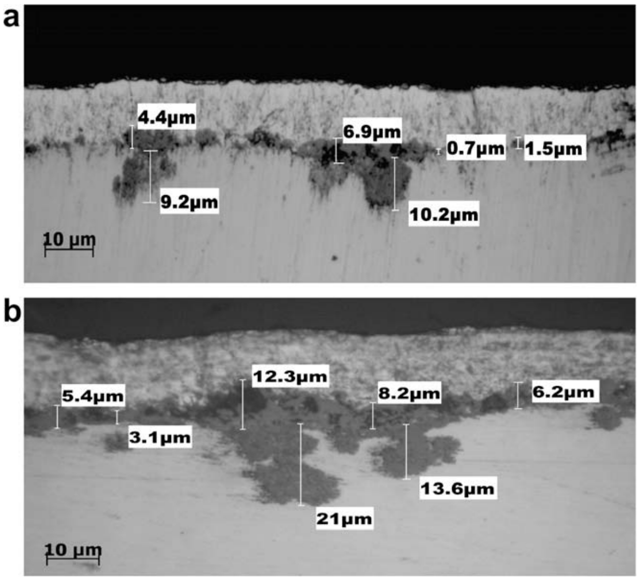

Fig. 4. Optical micrographs of the scales formed on Incoloy 800 samples after (a) 168 h (small cavities) and (b) 1440 h exposure at 873 K (larger cavities).

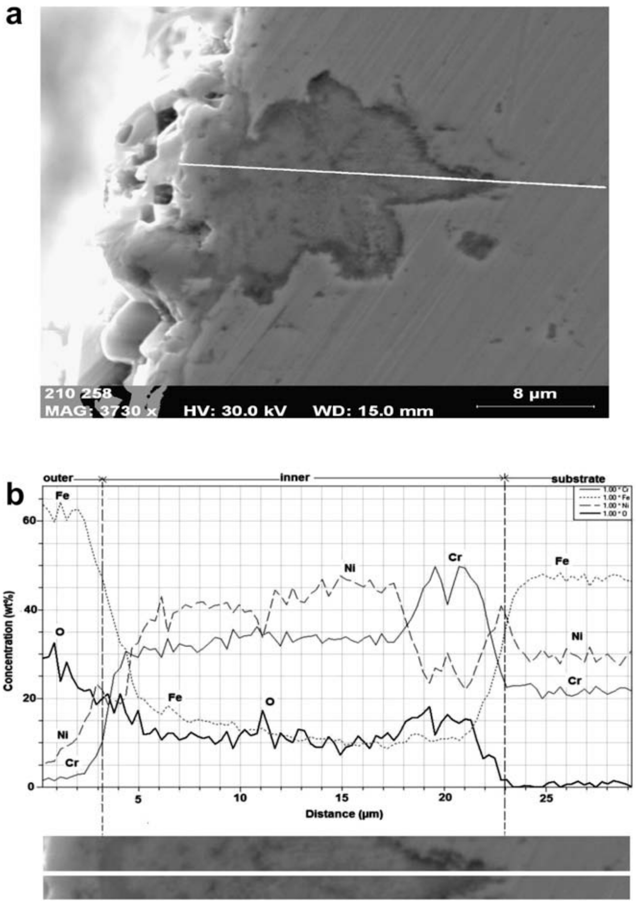

Fig. 5. (a) Cross-sectional SEM image of the Incoloy 800 after 1440 h exposure to water at 873 K and (b) the corresponding composition profile across the oxide thickness.

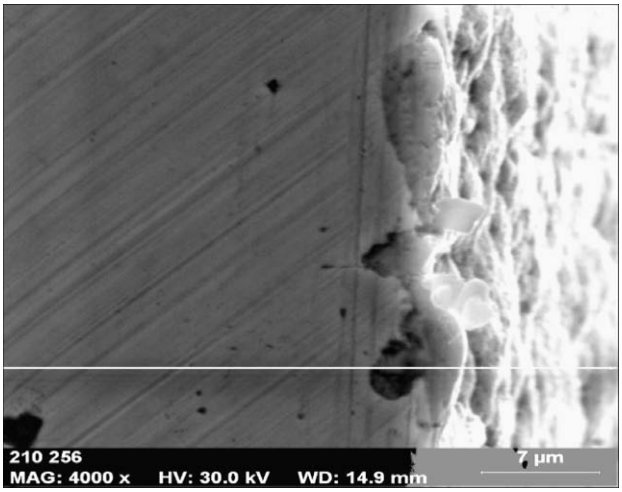

Fig. 6. Cross-sectional SEM image of the Incoloy 800 sample analyzed for 72 h by thermal gravimetric analysis.

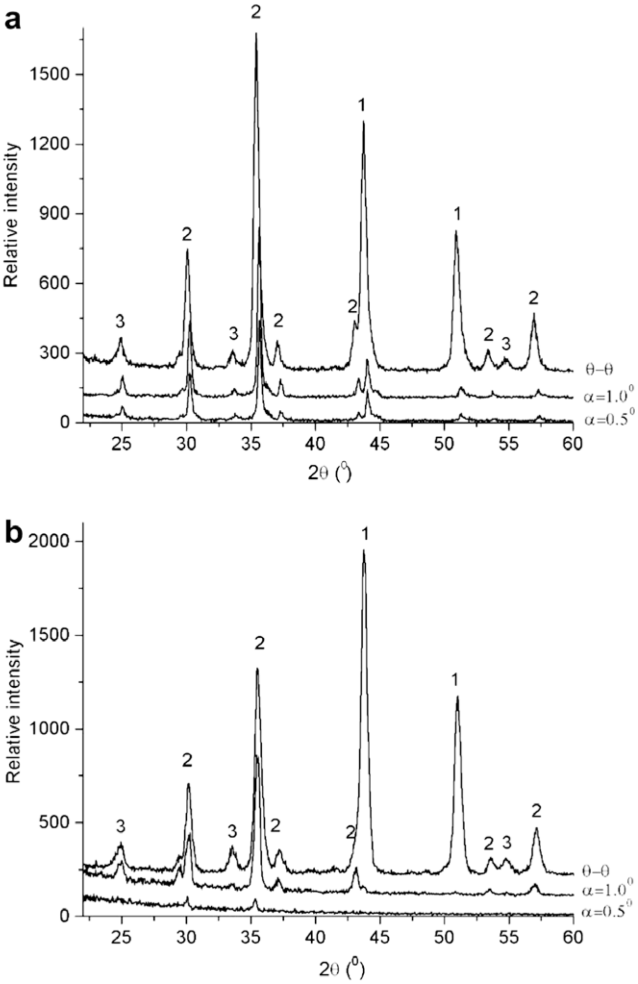

Fig. 7. X-ray diffraction patterns for Incoloy 800 tested at 873 K: (a) 168 h; (b) 1440 h where XRD peaks are 1 – for Incoloy 800; 2 – for $NiFe_2O_4$; 3 – XRD for $FeCrO_3$; note θ–θ XRD spectrum in symmetrical geometry.

for shorter times (0.7–6.9 μm outer layer and 10.2 μm inner layer) (see Fig. 4(a) and (b)). These thicknesses were measured for samples sections observed in optical microphotographs. In many micrographs, samples presented larger inner oxide layers than the outer oxide layers.

Fig. 5 shows the SEM cross-sectional morphology of the oxide layers formed on Incoloy 800 after exposure for 1440 h at 873 K, and corresponding composition versus depth profiles determined by EDS line-scans. This type of sample was used as an example because its oxide was thick enough to be analyzed. As shown in the elemental depth profile, there was Fe depletion in the inner oxide layer and enrichment in the outer oxide layer, whereas Ni and Cr were slightly more abundant in the inner oxide layer and depleted in the outer oxide layer. The Fe rich outer layer has a large grain size and seems porous. The inner layer enriched in Cr and Ni oxide corresponds to the cavities observed in the optical micrographs from Fig. 4 and is supposed to be representative of the internal oxidation zones. The thickness of the Fe rich external layer is about 4 μm and the thickness of the inner layer is about 19 μm. These values are comparable with the values obtained by optical microscopy. The internal oxidation layer may be expected to appear because the oxygen affinity for Cr is larger than for Fe, therefore Cr oxidizes more readily by reacting with diffused oxygen. Simultaneously the formation of this layer will decrease the oxygen potential at the oxide/metal interface making iron oxide less stable [8].

Another cross-sectional morphology of Incoloy 800 sample is presented in Fig. 6. This sample was tested for 72 h in steam at 823 K by thermal gravimetric analysis (TGA). This short test duration was designed to obtain information about factors which influence the appearance of the cavities. The TGA tests consisted of maintaining a sample in flowing steam with Ar for 72 h at a constant temperature (875 K) and atmospheric pressure. In this case the pressure was absent, but the oxygen content was high. As shown in Fig. 6, the sample presents cavities like those after autoclave exposure therefore it was assumed that the high temperature and high concentration of oxygen are responsible for internal oxidation of this alloy.

From XRD qualitative phase analysis, the following oxides were identified: $NiFe_2O_4$ and $FeCrO_3$. In Fig. 7 the XRD spectra obtained in symmetrical geometry and in asymmetrical geometry for incidence angle α of 0.5° and 1° are shown. On the surface of the sample exposed for 168 h at 873 K, a mixture of phases was observed, independent of the incidence angle value, indicating a single surface layer (Fig. 7(a)). For the sample oxidized at 873 K for 1440 h (Fig. 7(b)) the phases identified as a function of incidence angles indicated a double layer oxide: $NiFe_2O_4$ in the outer layer and $FeCrO_3$ in the inner layer.

The estimation of superficial layer characteristics has been performed by electrochemical impedance spectroscopy (EIS) method which does not accelerate the electrochemical reactions at metal/solution interface. Impedance spectra for Incoloy 800 are presented in Bode and Nyquist coordinates in Fig. 8. As shown in Bode plots the impedance values measured for samples tested 168 h are appreciable (near $10^4\ \Omega$) for oxides developed at 723, 773 and 823 K and slowly smaller for oxides developed at 873 K. Impedance magnitude (Z) is proportional to the oxide resistance (R) and inversely proportional with oxide capacity, so the larger the impedance value is, the better the corrosion resistance is. After 1440 h at 873 K, the impedance value slowly decreased and the oxide film developed under these conditions is not so corrosion resistant because of its enhanced porosity (Fig. 8, second column). The larger polarisation resistance values estimated from Nyquist plot extrapolation indicated a good corrosion resistance of the oxide films developed at 723 and 823 K after 1440 h (Table 3). For oxide films developed at 873 K after 1440 h exposure, the polarisation resistance is smaller compared to other oxides films. The polarisation resistance being inversely proportional with corrosion current density (according Buttler–Volmer equation), a smaller value of the polarisation resistance denotes a faster corrosion rate. Therefore, the oxide layer developed in supercritical water at 873 K after

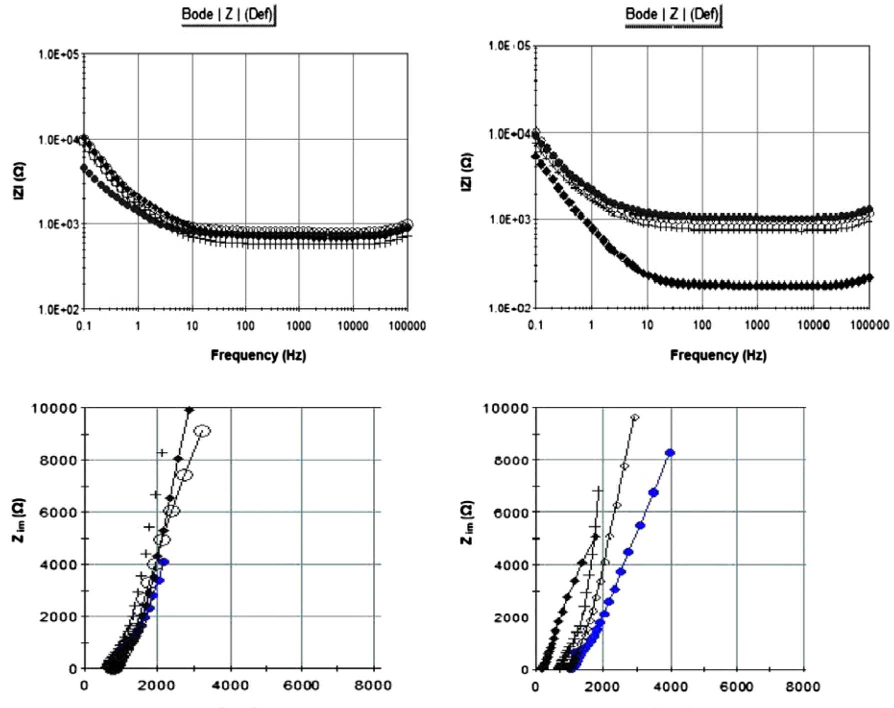

Fig. 8. Bode plots and Nyquist plots for Incoloy 800 samples oxidized at: (●) 723 K; (×) 773 K; (○) 823 K and (♦) 873 K for 168 h (first column) and for 1440 h (second column).

Table 3
Polarisation resistance (R_p) values for oxides estimated from Nyquist plot extrapolations.

Temperature (K)	R_p for oxides formed in 168 h (Ω)	R_p for oxides formed in 1440 h (Ω)
723	19000	33000
773	38000	34000
823	39000	47000
873	48000	22000

1440 h does not represent as good corrosion resistance as observed at lower temperatures.

4. Conclusions

The results of this corrosion study on Incoloy 800 tubes contribute to the data-base extension of nickel-based alloys oxide layer growth in supercritical water. A faster mass gain was observed with the increase of the testing temperature over more than 1000 h. At temperatures above 773 K oxidation follows parabolic rate kinetics, indicating that corrosion is driven by a diffusion process. Analysis results showed changes in the oxides chemical composition, microstructure and thickness versus testing conditions (pressure, temperature and time). The supercritical water exposure at 873 K for 1440 h resulted in thicker grain boundaries and in internal oxidation of this alloy. Based on the morphology and elemental concentration distribution, the oxide scale of the exposed samples could be divided into two distinct layers: an outer layer enriched in Fe oxide and an inner layer enriched in Cr and Ni oxides corresponding to small cavities supposedly due to internal oxidation. The external oxide films developed on Incoloy 800 at 873 K after 1440 h are more porous than oxides developed at 823, 773 and 723 K and present a weaker corrosion resistance.

Aknowledgment

This work was financially supported by the Romanian Program MATNANTECH CEEX-Contract 44/2005.

References

[1] K. Erlich, J. Konys, L. Heikinheimo, J. Nucl. Mater. 327 (2004) 140.
[2] G.S. Was, S. Teysseyre, J. McKinley, Corrosion and stress corrosion cracking of iron and nickel-based austenitic alloys in supercritical water, in: Proceeding NACE's Annual Conference, Corrosion, New Orleans LA, Paper 04492, 2004.
[3] L. Tan, K. Sridharan, T.R. Allen, J. Nucl. Mater. 348 (2006) 263.
[4] W.E. Ruther, R.R. Schlueter, R.H. Lee, R.K. Hart, Corrosion 22 (1966) 147.
[5] A. Fry, S. Osgerby, M. Wright, Oxidation of Alloys in Steam Environments, NPL Report, MATC (A) 90, 2002.
[6] A.M. Iglesias, M.A.C. Raffo Calderon, Thermal resistance of oxides growth on Incoloy 800 steam generator tubes, Nucl. Eng. Design 219 (1) (2003) 1–10.
[7] D. Squarer, Minutes of The Fifth HPLWR Project Meeting of 29–31 July 2002 at FZK – Karlsruhe, Germany, Forschungszentrum Karlsruhe, Germany, HPLWR-M 11, September 2002 (RE).
[8] X. Ren, K. Sridharan, T.R. Allen, J. Nucl. Mater. 358 (2/3) (2006) 227.